

Orbital evolution of a planet on an inclined orbit interacting with a disc

Jean Teyssandier^{1*}, Caroline Terquem^{1†} and John C. B. Papaloizou^{2‡}

¹ *Institut d'Astrophysique de Paris, UPMC Univ Paris 06, CNRS, UMR7095, 98 bis bd Arago, F-75014, Paris, France*

² *Department of Applied Mathematics and Theoretical Physics, University of Cambridge, Centre for Mathematical Sciences, Wilberforce Road, Cambridge, CB3 0WA, UK*

2012

ABSTRACT

We study the dynamics of a planet on an orbit inclined with respect to a disc. If the initial inclination of the orbit is larger than some critical value, the gravitational force exerted by the disc on the planet leads to a Kozai cycle in which the eccentricity of the orbit is pumped up to large values and oscillates with time in antiphase with the inclination. On the other hand, both the inclination and the eccentricity are damped by the frictional force that the planet is subject to when it crosses the disc. We show that, by maintaining either the inclination or the eccentricity at large values, the Kozai effect provides a way of delaying alignment with the disc and circularization of the orbit. We find the critical value to be characteristically as small as about 20 degrees. Typically, Neptune or lower mass planets would remain on inclined and eccentric orbits over the disc lifetime, whereas orbits of Jupiter or higher mass planets would align and circularize. This could play a significant role in planet formation scenarios.

Key words: celestial mechanics — planetary systems — planetary systems: formation — planetary systems: protoplanetary discs — planets and satellites: general

* Email: teyssand@iap.fr

† E-mail: caroline.terquem@iap.fr

‡ E-mail: J.C.B.Papaloizou@damtp.cam.ac.uk

1 INTRODUCTION

At the time of writing, more than 800 extrasolar planets have been detected around main sequence stars. Most of these objects have been observed through radial velocity measurements, and about one third of them have also been detected through transit measurements. In addition, the Kepler mission has so far released about 2300 planet candidates (Borucki et al. 2011, Batalha et al. 2012). Only a few of these objects have been confirmed by radial velocity measurements so far, but the number of false positive is expected to be very small. The rate at which extrasolar planets are being discovered is accordingly increasing very sharply.

The angle between the sky projections of the stellar spin axis and the orbit normal (that we will call hereafter the *projected inclination angle*) has been measured using the Rossiter–McLaughlin effect for 53 planets (Albrecht et al. 2012 and references therein). About one third display significant misalignment with retrograde orbits being indicated in some cases. Misalignment, therefore, is common, at least for short period systems for which measurements have been made. Note however that the planets in this sample are rather massive. The lightest one has a mass of about 25 earth masses, whereas the other planets in the sample have masses ranging from a few tenths of a Jupiter mass to several Jupiter masses. By performing duration ratio statistics on the Kepler planetary candidates, Fabrycky et al. (2012) have concluded that pairs of planets in their sample are aligned to within a few degrees. As the Kepler catalog contains a majority of super–earth and Neptune–like planets, it is possible that misalignment is less common for lower mass planets.

According to the commonly accepted core accretion scenario, in which planets form in a disc through the accretion of solid material into a core followed, in the case of giant planets, by the capture of a gaseous atmosphere, the orbit of planets should lie in the disc, and therefore in the equatorial plane of the star. In this model, migration due to tidal interaction between disc and planets can be invoked to explain the presence of giant planets on very short orbits. However, such an interaction would not account for the occurrence of any inclination of the orbit. Therefore, this scenario is not likely to apply to the hot Jupiters that are observed to be on inclined orbits. Planet formation through fragmentation of the disc might be considered, but in that case the orbits are also expected to lie in the plane of the disc.

One scenario that has been proposed for misaligning the orbits of hot Jupiters that have

formed in a disc lying in the stellar equatorial plane relies on gravitational interaction with a distant stellar or planetary companion that takes place after the disc has dissipated. When the two orbits are not coplanar, the secular perturbation exerted by the companion produces a Kozai cycle in which the eccentricity and the inclination of the inner planet's orbit vary in antiphase. If the pericenter distance gets small enough, the orbit may become circularized because of the tidal interaction with the central star, and the orbit shrinks while, in some circumstances, keeping a high inclination (Fabrycky & Tremaine 2007, Wu et al. 2007, Naoz et al. 2011). In this model, a distant companion is needed which, however, may not always be present in reality. Other models rely on planet–planet scattering (Chatterjee et al. 2008) or secular chaos (Wu & Lithwick 2011).

It has been proposed that the disc itself may be misaligned with respect to the stellar equatorial plane. That could happen if the disc, at later times, were accreting material with angular momentum misaligned with that of the star, as considered by Bate et al. (2010). If at that stage there was enough mass in the disc to form planets, their orbits would naturally be inclined with respect to the stellar equatorial plane. A similar scenario was studied by Thies et al. (2011), who pointed out that close encounters of a disc accreting from an extended envelope with another star could result in the disc plane becoming tilted, possibly even to a retrograde orientation with respect to its original one. Planetary orbits inclined with respect to the stellar equatorial plane would also result if the stellar spin axis were tilted due to interaction with the disc (Lai et al. 2011, Foucart & Lai 2011). Note however that, by comparing stellar rotation axis inclination angles with the geometrically measured disc inclinations for a sample of eight debris-discs, Watson et al. (2011) have seen no evidence for a misalignment between the two.

Another possibility would be that the misaligned planets have formed out of the disc through a fragmentation process occurring in the protostellar envelope while it collapses onto the protostar, as envisioned by Papaloizou & Terquem (2001) and Terquem & Papaloizou (2002). In this scenario, a population of planetary objects form rapidly enough that their orbits can undergo dynamical relaxation on a timescale on the order of a few 10^4 years. During the relaxation process, most of the objects are ejected, while one to a few planets become more bound to the central star. Formation of hot Jupiters through tidal circularization by the central star of a highly eccentric orbit may occur (Papaloizou & Terquem 2001). The orbits of the planets that are left in the system at the end of the relaxation process display a range of eccentricities and inclinations (Adams & Laughlin 2003). In this context,

the misaligned planets interact with the disc that has formed around the star during the protostellar envelope collapse. It is the subsequent dynamics of a system of this type, consisting of a gaseous disc together with a planet with an orbital plane misaligned with its midplane that we propose to investigate here. Note that we do not expect low mass planets to form according to the scenario of Papaloizou & Terquem (2001). On the other hand, in the scenario proposed by Bate et al. (2010), it may happen that subsequent discs with different inclinations form and dissipate, so that planets formed early in a disc may interact at later time with a disc with different orientation.

In the present paper, we focus on a system with only one planet. Multiple systems will be studied in future publications. Some preliminary work on the interaction of a planet on an inclined orbit with a disc has been carried out by Terquem & Ajmia (2010). It was found that the gravitational force exerted by the disc onto the planet leads to a Kozai cycle in which the eccentricity and the inclination of the orbit vary periodically with large amplitudes. This indicates that a planet's orbit which is inclined to start with may achieve high eccentricity. In their calculations, Terquem & Ajmia (2010) adopted a two dimensional flat disc model and ignored the frictional force felt by the planet as it passes through the disc. In the present paper, we extend this work by modelling the disc in three dimensions and including the frictional force. Our goal is to understand under what circumstances inclined orbits can be maintained when the disc is present. We consider planets with masses ranging from Neptune mass to several Jupiter masses. The plan of the paper is as follows:

In section 2.1, we describe the three dimensional disc model used in the numerical simulations and the calculation of the gravitational force exerted by the disc on a planet in an inclined orbit. A computationally convenient formulation, in terms of elliptic integrals, is presented in an appendix. We go on to give a brief review of the Kozai mechanism in section 2.2. In section 2.3, we give an expression for the frictional force exerted by the disc on the planet, and derive a damping timescale based on a simplified analysis in section 2.4. In section 3, we present the results of numerical simulations of the interaction between a planet on an inclined orbit and a disc. We first perform simulations without the frictional force in section 3.1 and compare the results to those of Terquem & Ajmia (2010) that were obtained for a two dimensional flat disc model. In section 3.2, we include friction. We show that, when the planet's orbit starts with a low inclination (less than about 23°) with respect to the disc, it becomes aligned with the disc plane and circularized by the frictional force. However, when the inclination is initially high enough, the Kozai effect is present.

This pumps up the eccentricity of the planet's orbit maintaining either the inclination or the eccentricity at large values. As a consequence, alignment of the orbital and disc planes, as well as circularization of the orbit resulting from the frictional force, is delayed. In some cases, the orbit stays misaligned over the disc lifetime. More massive planets and planets further away from the star align faster. In addition, more massive discs favour alignment. In section 4, we discuss our results in the light of the observations that have been reported so far.

2 INTERACTION BETWEEN A PLANET ON AN INCLINED ORBIT AND A DISC

2.1 Gravitational potential and disc model

We consider a planet of mass M_p orbiting around a star of mass M_\star which is itself surrounded by a disc of mass M_d . The disc's midplane is in the equatorial plane of the star whereas the orbit of the planet is inclined with respect to this plane. We denote by I the angle between the orbital plane and the disc's plane. We suppose that the angular momentum of the disc is large compared to that of the planet's orbit so that the effect of the planet on the disc is negligible: the disc does not precess and its orientation is invariable (see appendix A). We denote by (x, y, z) the Cartesian coordinate system centred on the star and (r, φ, z) the associated cylindrical coordinates. The (axisymmetric) disc is in the (x, y) -plane, its inner radius is R_i , its outer radius is R_o and its thickness (defining the region within which the mass is confined) at radius r is $2H(r)$.

The gravitational potential exerted by the disk at the location (r, z) of the planet is:

$$\Phi(r, z) = -G \int_{R_i}^{R_o} \int_{-H}^H \int_0^{2\pi} \frac{\rho(r', z') r' dr' dz' d\phi'}{\sqrt{r^2 + r'^2 - 2rr' \cos \phi' + (z - z')^2}}, \quad (1)$$

where G is the gravitational constant and ρ is the mass density in the disc.

We assume that ρ falls off exponentially with z^2 near the midplane with a cut off at $|z| = H(r)$, while decreasing as a power of r . Thus we adopt:

$$\rho(r, z) = \left[e^{\frac{1}{2}(1-z^2/H(r)^2)} - 1 \right] \left(\frac{r}{R_o} \right)^{-n} \frac{\rho_0}{e^{1/2} - 1}, \quad (2)$$

where ρ_0 is a constant. We have $\rho = 0$ at the surface of the disc, i.e. when $|z| = H$, and $\rho(r, 0) = \rho_0(r/R_o)^{-n}$ in the midplane. This z -dependence of ρ has been chosen for simplicity,

but we note that the details of how ρ varies with z do not matter. What is important is the local disc surface density at the location the planet passes through. This largely determines the change in orbital energy resulting from the dynamical drag force (as is apparent from equation (11) of section 2.3 below).

The mass density given above is discontinuous at $r = R_i$ and $r = R_o$, as ρ is zero outside the disc. We have found that this could introduce some numerical artefacts in the calculation of the disc's gravitational force, so that in some runs we have replaced ρ by $\rho \times f(r)$ with:

$$f(r) = \left[1 - \left(\frac{R_i}{r} \right)^{10} \right] \left[1 - \left(\frac{r}{R_o} \right)^{20} \right]. \quad (3)$$

The exponents 10 and 20 ensure that the edges are rather sharp, so that we get quantitatively the same orbital evolution whether the factor f is used or not.

In the calculations presented below, we chose a value of the disc mass M_d and calculate ρ_0 using $M_d = \int \int_{disc} \rho dV$. For the disc's semithickness, we chose a constant aspect ratio:

$$H(r) = H_0 r, \quad (4)$$

where H_0 is a constant. The gravitational force per unit mass exerted by the disc onto the planet is $-\nabla\Phi$. In appendix B, we give convenient expressions for $-\nabla\Phi$ in terms of elliptic integrals which can be readily computed.

2.2 The Kozai mechanism

The Kozai effect (Kozai 1962, Lidov 1962) arises when an inner body on an inclined orbit is perturbed by a distant companion. First derived by Kozai to study the motion of inclined asteroids around the Sun under perturbations from Jupiter, it has since found many applications in astrophysics. We are interested here in cases where the inner body is a planet of mass M_p . We denote a its semimajor axis, M' the mass of the outer companion, assumed to be on a circular orbit, and a' its semimajor axis. We consider the case $a' \gg a$. The secular perturbation from the outer companion causes the eccentricity e of the inner planet and the mutual inclination I of the two orbits to oscillate in time in antiphase provided that the initial inclination angle I_0 is larger than a critical angle I_c given by:

$$\cos^2 I_c = \frac{3}{5}. \quad (5)$$

The maximum value reached by the eccentricity is then given by:

$$e_{\max} = \left(1 - \frac{5}{3} \cos^2 I_0\right)^{1/2}, \quad (6)$$

and the time t_{evol} it takes to reach e_{\max} starting from e_0 is (Innanen et al. 1997):

$$\frac{t_{\text{evol}}}{\tau} = 0.42 \left(\sin^2 I_0 - \frac{2}{5}\right)^{-1/2} \ln \left(\frac{e_{\max}}{e_0}\right), \quad (7)$$

with the time τ defined by:

$$\tau = \left(\frac{a'}{a}\right)^3 \left(\frac{M_\star}{M'}\right) \frac{T}{2\pi}, \quad (8)$$

where T is the orbital period of the inner planet. If the eccentricity oscillates between e_{\min} and e_{\max} , then the period of the oscillations P_{osc} is given by $P_{\text{osc}} = 2t_{\text{evol}}$ with $e_0 = e_{\min}$ in equation (7).

Since the two orbits are well separated, the component of the angular momentum of the inner orbit perpendicular to the orbital plane is constant. As it is proportional to $\sqrt{1 - e^2} \cos I$, the oscillations of I and e are in antiphase. Hereafter, we will refer to this mechanism as the *classical Kozai effect*.

Terquem & Ajmia (2010) found that the Kozai effect extends to the case where the inner orbit is perturbed by the gravitational potential of a disc, even when the orbit of the planet crosses the disc, provided most of the disc mass is beyond the planet's orbit. In that case, I is the angle between the orbital plane and the disc's plane. They also showed that, in agreement with equations (7) and (8), the period of the oscillations decreased with a . It was also found to decrease with increasing disc mass. When the semimajor axis of the planet is small compared to the disc's inner radius, the evolution timescale is of the same form as that given by equation (7) but with

$$\tau \propto \left(\frac{R_o}{a}\right)^3 \left(\frac{M_\star}{M_d}\right) \frac{T}{2\pi}, \quad (9)$$

where the coefficient of proportionality depends on the functional form of ρ and on the ratio R_i/R_o .

2.3 Friction

When the planet crosses the disc, as it has a relative velocity with respect to the particles in the disc, it suffers a frictional force. There are two types of drag acting on the planet: (i) an aerodynamic drag, due to the fact that the planet has a finite size and suffers direct collisions

with the particles in the disc, and (ii) a dynamical drag, due to the fact that particles in the disc are gravitationally scattered by the planet.

Adopting a drag coefficient of unity, the aerodynamic drag force per unit mass exerted on the planet located at (r, φ, z) , or equivalently (x, y, z) , can be written as:

$$\mathbf{\Gamma}_{\text{aero}} = -\frac{1}{2M_p} \pi R_p^2 \rho(r, z) v_{\text{rel}} \mathbf{v}_{\text{rel}}, \quad (10)$$

where R_p is the planet's radius and \mathbf{v}_{rel} is the relative velocity of the planet with respect to the particles in the disc at the location (x, y, z) . If we denote $\mathbf{v} = (v_x, v_y, v_z)$ the velocity of the planet, then $\mathbf{v}_{\text{rel}} = (v_x + y\Omega, v_y - x\Omega, v_z)$, where $\Omega = \sqrt{GM_\star/r^3}$.

The dynamical drag is the gravitational force exerted by the particles in the disc on the planet that is associated with the scattering and change of location that occurs as a result of the passage of the planet. The main contribution to this force comes from the particles located in the vicinity of the planet at the time it crosses the disc. Note that the gravitational force from these particles has already been included in $-\nabla\Phi$ (see section 2.1), but as we have ignored the motion of the particles in the disc relative to the planet when calculating this force it is conservative and does not capture the change of energy of the planet's orbital motion. The problem is similar to dynamical friction in a collisionless medium (e.g., Binney & Tremaine 1987).

When the inclination angle of the planet's orbit with respect to the disc is not very small, $v_{\text{rel}} \sim \sqrt{GM_\star/a}$, with a being the semimajor axis of the planet's orbit, is supersonic. In this case, the dynamical friction force per unit mass acting on the planet can be written as (Ruderman & Spiegel 1971, Rephaeli & Salpeter 1980, Ostriker 1999):

$$\mathbf{\Gamma}_{\text{dyn}} = -4\pi G^2 M_p \rho(r, z) \left| \ln \frac{H(r)}{R_p} \right| \frac{\mathbf{v}_{\text{rel}}}{v_{\text{rel}}^3}. \quad (11)$$

The ratio of the two frictional forces is thus:

$$\frac{\Gamma_{\text{aero}}}{\Gamma_{\text{dyn}}} \sim \frac{1}{8 \left| \ln \frac{H(r)}{R_p} \right|} \left(\frac{R_p}{a} \right)^2 \left(\frac{M_\star}{M_p} \right)^2, \quad (12)$$

where we have replaced v_{rel}^2 by GM_\star/a . In this paper, we will focus on planets with masses at least that of Neptune, for which the previous expression gives $\Gamma_{\text{aero}}/\Gamma_{\text{dyn}} \ll 1$ for the orbital parameters we consider. Therefore, friction is dominated by the dynamical term even though a large value of unity was adopted for the drag coefficient.

2.4 Evolution timescale

The velocity v of the planet is, in first approximation, the Keplerian velocity around the star, i.e. $v \simeq \sqrt{GM_\star/a}$. To simplify matters, we approximate the relative velocity by its vertical component so that $v_{\text{rel}} \sim v_z \simeq v \sin I \simeq \sqrt{GM_\star/a} \sin I$.

When the planet's orbit has a significant eccentricity, the relative velocity is in general larger as the planet crosses the disc closer to pericenter than apocenter and its horizontal components (in the disc's plane) are then important. We define a damping timescale for the planet in the absence of forces other than friction as:

$$\tau_{\text{damp}} = \left(\frac{1}{v} \frac{dv}{dt} \right)^{-1} = \frac{v}{\Gamma_{\text{dyn}}}. \quad (13)$$

This is the characteristic timescale on which the frictional force Γ_{dyn} damps the velocity of the planet. Note that $\tau_{\text{damp}} = 2a(da/dt)^{-1}$. With the above approximation for v_{rel} and $|\ln(H/R_p)| \simeq 6$, which corresponds to giant planets at around 10 au in a disc with $H(r) = 2.5 \times 10^{-2}r$, as we consider below in the numerical calculations, we get:

$$\tau_{\text{damp}} \sim \frac{M_\star^2 \sin^2 I}{24\pi M_p a^3 \rho(r, z)} \frac{T}{2\pi}, \quad (14)$$

where T is the orbital period of the planet.

To proceed further, for the purpose of getting a convenient analytical estimate of τ_{damp} , we approximate the vertical dependence of the mass density by a δ -function in z and set $\rho(r, z) = 2\delta(z)H(r)\rho_0(r/R_o)^{-n}$. Then we get $\Sigma(r) = \int_{-H}^H \rho(r, z)dz = 2\rho_0(r/R_o)^{-n}H(r)$. Using equation (4), we can then calculate the disc mass to be $M_d = \int_{R_i}^{R_o} \Sigma(r)2\pi r dr \simeq 8\pi\rho_0 H_0 R_o^3/3$, where we have used $n = 3/2$, as in the numerical simulations below. That allows us to express ρ_0 in term of M_d , such that $\rho_0 \simeq 3M_d/(8\pi H_0 R_o^3)$. In accordance with equation (2), we identify the midplane mass density as $\rho(r, 0) = \rho_0(r/R_o)^{-n} \simeq 3M_d(r/R_o)^{-n}/(8\pi H_0 R_o^3)$. We now suppose that the planet's orbit is not too eccentric so that ρ can be evaluated at $r = a$ in the expression of τ_{damp} . Finally, equation (14) gives:

$$\tau_{\text{damp}} \sim \frac{M_\star^2}{9M_p M_d} \left(\frac{R_o}{a} \right)^{3/2} H_0 \sin^2 I \frac{T}{2\pi}. \quad (15)$$

This expression may not give the correct quantitative value of the damping timescale, because of the approximations that have been used in deriving it, but it gives the scaling of τ_{damp} with the different parameters. Also, although the dependence on the eccentricity has

not been taken into account in this expression, as pointed out above, we expect the damping timescale to be larger when the eccentricity is larger.

3 NUMERICAL SIMULATIONS

To study the evolution of the system (star, planet, disc), we use the N -body code described in Papaloizou & Terquem (2001) in which we have added the gravitational and frictional forces exerted by the disc on the planet.

The equation of motion for the planet is:

$$\frac{d^2\mathbf{r}}{dt^2} = -\frac{GM_\star\mathbf{r}}{|\mathbf{r}|^3} - \nabla\Phi + \mathbf{\Gamma}_{\text{aero}} + \mathbf{\Gamma}_{\text{dyn}} + \mathbf{\Gamma}_{t,r} - \frac{GM_p\mathbf{r}}{|\mathbf{r}|^3}. \quad (16)$$

The last term on the right-hand side is the acceleration of the coordinate system based on the central star. It arises because the center of mass of the system does not coincide with that of the star. This term takes into account only the force exerted by the planet onto the star, and neglects the net force of the disc on the central star, which would of course require a calculation of the disc response to the planet's perturbation. Tides raised by the star in the planet and relativistic effects are included through $\mathbf{\Gamma}_{t,r}$, but they are unimportant here as the planet does not approach the star closely. Equation (16) is integrated using the Bulirsch–Stoer method. The integrals over ϕ involved in $\nabla\Phi$ are calculated using elliptic integrals (see appendix B). The integrals over r and z are calculated with the Romberg method (Press et al. 1993).

The planet is set on a circular orbit at the distance r_p from the star. When the planet does not pass through the disc, e.g. when there is no friction, the orbital energy is conserved and r_p is equal to the planet's semimajor axis a throughout the evolution of the system. The initial inclination angle of the orbit with respect to the disk is I_0 . In the simulations reported here, we have taken $M_\star = 1 M_\odot$, a radial power law with exponent $n = 3/2$ for the disc mass density ρ (see eq. [2]), a disc aspect ratio $H_0 = 2.5 \times 10^{-2}$ and a disc outer radius $R_o = 100$ au.

We will consider a planet with either (i) $M_p = 10^{-3} M_\odot \equiv 1 M_J$ and $R_p = 7 \times 10^9$ cm (Jupiter), (ii) $M_p = 5 \times 10^{-5} M_\odot \equiv 1 M_N$ and $R_p = 2.5 \times 10^9$ cm (Neptune), (iii) $M_p = 10^{-2} M_\odot = 10 M_J$ and $R_p = 8.4 \times 10^9$ cm, i.e. 1.2 times Jupiter's radius. These latter values approximately correspond to the mass and radius of the planet XO-3 b, which has been detected both in transit and using radial velocity measurements (Johns–Krull et al. 2008, Winn et al. 2008).

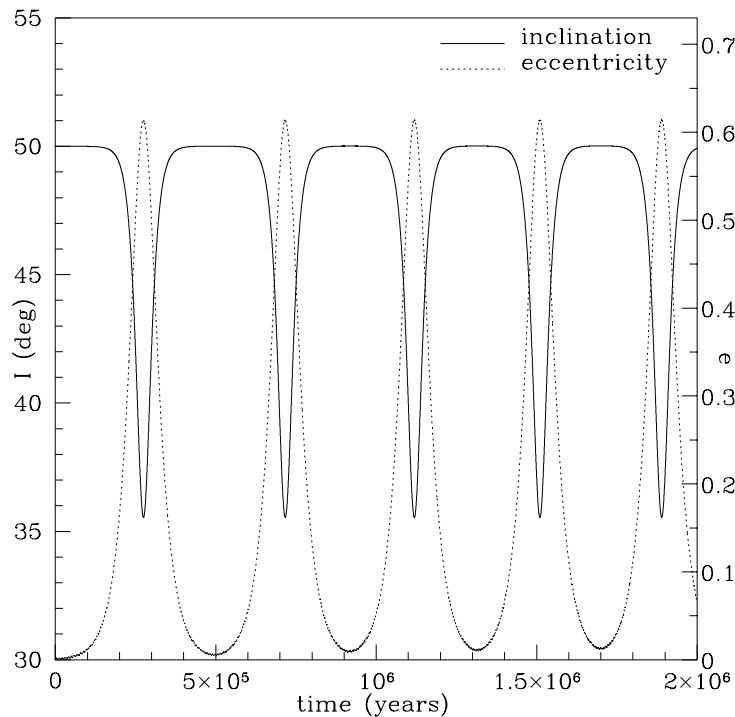


Figure 1. Eccentricity e (dotted line) and inclination angle I (in degrees, solid line) versus time (in yr) in the absence of friction for $M_p = 1 M_J$, $r_p = 5$ au, $M_d = 10^{-2} M_\odot$, $R_i = 10$ au and $I_0 = 50^\circ$.

3.1 Gravitation only

To get a benchmark, we first consider the evolution of the planet's orbit in the case where friction is ignored (i.e. Γ_{aero} and Γ_{dyn} are set to zero in eq. [16]). This applies when the planet's distance to the star is at all times smaller than the disc inner radius (e.g., planet orbiting in a cavity). These calculations are similar to those performed by Terquem & Ajmia (2010) and a comparison is made below.

Figure 1 shows the time evolution of the eccentricity e and inclination I for $M_p = 1 M_J$, $r_p = 5$ au, $M_d = 10^{-2} M_\odot$, $R_i = 10$ au and $I_0 = 50^\circ$.

The inclination angle varies between $I_{\min} = I_c$ and I_{\max} , where I_c is the critical value of I_0 below which eccentricity growth is not observed. The fact that $I_{\min} = I_c$ is illustrated in figure 2, which shows the time evolution of the inclination I for $M_p = 1 M_J$, $r_p = 7$ au, $M_d = 10^{-2} M_\odot$, $R_i = 1$ au and I_0 varying between 23° and 50° . For these parameters, oscillations of the eccentricity and inclination disappear once I_0 becomes smaller than 23° , which means that $I_c = 23^\circ$. For values of I_0 well above I_c , the inclination is seen to oscillate between $I_{\min} = I_c$ and I_{\max} . When I_0 decreases however, the amplitude of the oscillations is such that I_{\min} gets a bit larger than I_c .

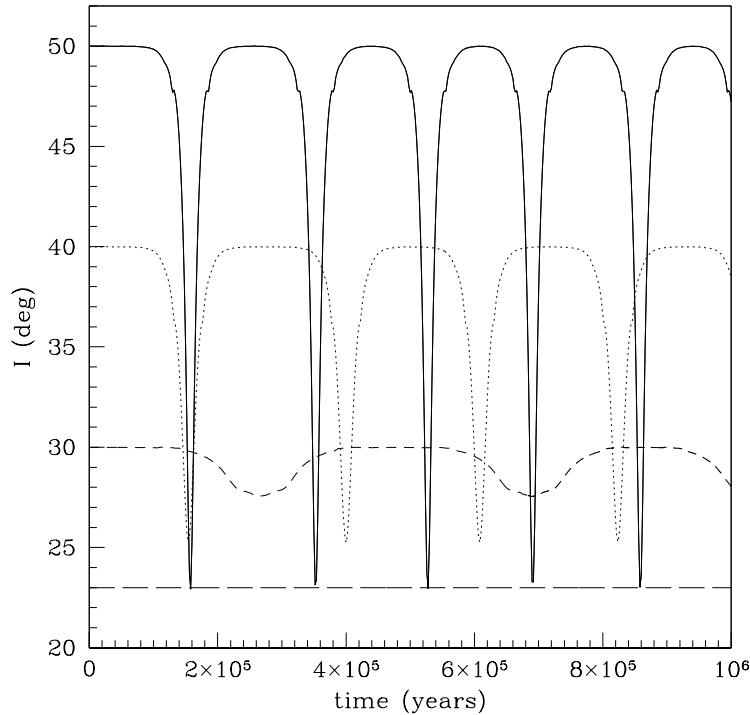


Figure 2. Inclination I (in degrees) versus time (in yr) in the absence of friction for $M_p = 1 M_J$, $r_p = 7$ au, $M_d = 10^{-2} M_\odot$, $R_i = 1$ au and $I_0 = 50^\circ$ (solid line), 40° (dotted line), 30° (short-dashed line) and 23° (long-dashed line). For these parameters, $I_c = 23^\circ$. No oscillations are present for $I_0 < I_c$.

As already noted by Terquem & Ajmia (2010), since I_c depends on the gravitational force exerted onto the planet, it varies with the initial position of the planet r_p . When $r_p \ll R_i$, the conditions are similar to the classical Kozai effect and the gravitational force from the disc can be approximated by a quadrupole term. In this case, it can be shown that $I_c = 39^\circ$ (eq. [5]). When r_p is larger though, the quadrupole approximation is not valid anymore and I_c gets smaller. This is illustrated in figure 3, which shows the critical angle I_c as a function of r_p , which here is the same as the planet's semimajor axis since the orbit is initially circular and there is no energy dissipation. These calculations are done for $M_p = 1 M_J$, $M_d = 10^{-2} M_\odot$, $R_i = 10$ au and r_p varying between 1 and 35 au. For these parameters, the Kozai effect disappears when r_p becomes larger than ~ 40 au, as most of the mass is then no longer outside the orbit of the planet (Terquem & Ajmia 2010).

For comparison, we have also run the case displayed in figure 1 by modelling the disc in two dimensions only, as in Terquem & Ajmia (2010). The gravitational potential is then calculated as arising from a distribution of mass with surface density $\Sigma_{2D}(r) \propto r^{-p}$. We take $p = 1/2$ as in the 3D calculations we have $\Sigma(r) \sim \rho(r)H(r) \propto r^{-1/2}$. There is very good

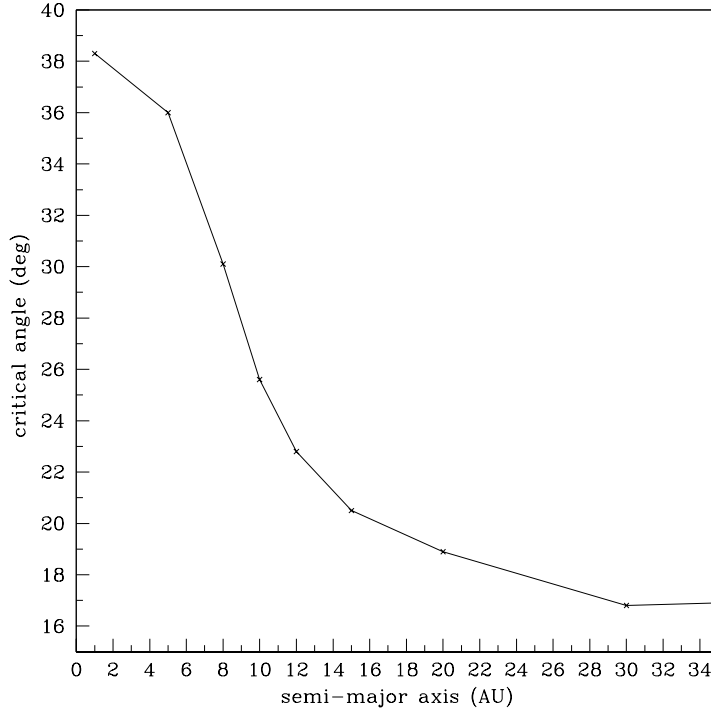


Figure 3. I_c (in degrees) versus r_p (in au) in the absence of friction for $M_p = 1 M_J$, $M_d = 10^{-2} M_\odot$, $R_i = 10$ au and r_p varying between 1 and 35 au. For $r_p \ll R_i$ au we recover the classical Kozai value $I_c = 39^\circ$.

agreement between the two sets of calculations. The extrema of I and e and the period of the oscillations are roughly the same.

In the 3D case, we have also checked that the vertical structure of the disc does not affect the oscillations. Indeed, when the disc mass is kept constant but H_0 is varied in equation (4), the oscillations are unchanged.

3.2 The effect of friction

We are now going to study the effect of friction on the evolution of the planet's orbit by taking into account Γ_{aero} and Γ_{dyn} in equation (16).

Figure 4 shows the time evolution of the orbital parameters I , e , semimajor axis a and distance to pericenter $a(1 - e)$ for $M_p = 1 M_N$, $r_p = 7$ au, $M_d = 10^{-2} M_\odot$, $R_i = 1$ au and for two different values of I_o . For these parameters, $I_c = 23^\circ$ (the critical angle does not depend on the mass of the planet and therefore is the same as in fig. 2). As discussed in section 2.4, the damping timescale increases with I and e . Therefore, when $I_o > I_c$, as at all times one of these parameters has a large value because of the Kozai cycle, the damping timescale is longer than in the case $I_o < I_c$ and $e = 0$. This is illustrated in figure 4, where we see that a decreases much more rapidly when $I_o = 20^\circ$ than when $I_o = 50^\circ$. In the

case where there is no Kozai cycle, the orbit stays circular and I is damped faster as it becomes smaller, so that the orbit aligns with the disc on a very short timescale. When $I_o > I_c$, Kozai oscillations are present as expected, but the oscillations are damped because of friction. We observe that damping is much less efficient than in the $I_o = 20^\circ$ case, even though the inclination I does reach values that are not much larger than 20° and for which the damping timescale would be similar if the orbit were circular. When the Kozai cycle is present though, the eccentricity of the orbit is large when I is minimum, which results in the damping timescale being maintained at large values. Contrary to what happens when $I_o < I_c$ then, the damping timescale stays roughly constant. This is illustrated in the plot of figure 4 that shows a versus time. Ultimately, if the disc were present long enough, the orbit of the planet would align with the disc and would be circularized (I and e vanish). For a Neptune mass planet and the parameters used here though, we find that misalignment can be maintained over the the disc lifetime, which is of a few million years. A Jupiter mass planet would align faster, as discussed below.

These calculations show that, by pumping up the eccentricity of the planet's orbit and maintaining either I or e at large values, the Kozai effect provides a way of delaying alignment with the disc and circularization of the orbit.

We see in figure 4 that the period of the oscillations decreases with time. If there were no dissipation, this period would stay constant. In the classical Kozai cycle, when the orbit of the inner planet has a semimajor axis a , the time it takes to reach e_{\max} starting from e_{\min} , is proportional to $a^{-3/2} \ln(e_{\max}/e_{\min})$ (see eq. [7] and [8]). Although this formula has been derived for a quadrupolar gravitational potential, it may be expected to give a general trend in the disc case as well. Friction reduces a , which tends to increase this timescale. But the amplitude of the cycle also decreases (e_{\min} increases and e_{\max} decreases), so that the net effect is a shorter timescale.

As pointed out in section 2.3, the expression for dynamical friction given by equation (11) is valid only when the relative velocity of the planet with respect to the particles in the disc is supersonic. This is not the case when I is close to zero and, therefore, the part of the curves in figure 4 corresponding to I close to zero can be interpreted only qualitatively.

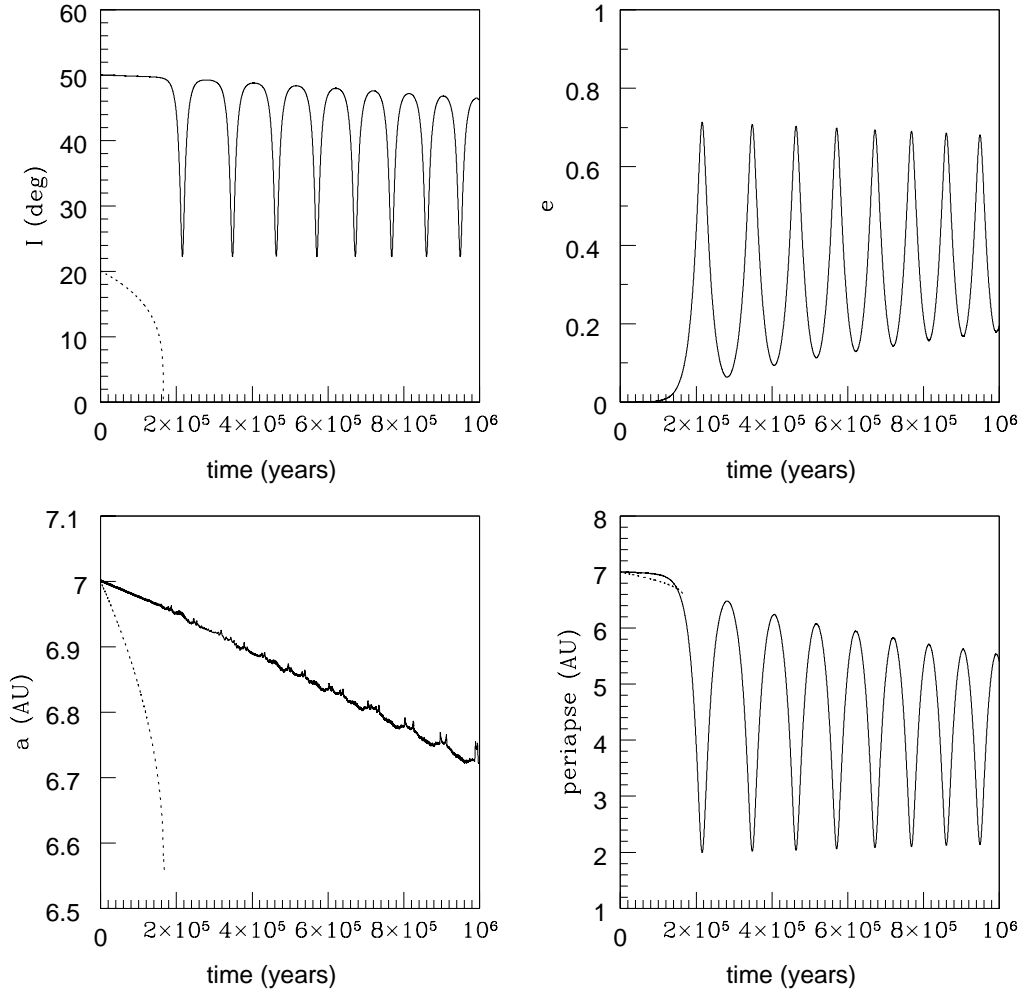


Figure 4. Inclination I (in degrees, upper left plot), eccentricity e (upper right plot), semimajor axis a (in au, lower left plot) and pericenter distance $a(1 - e)$ (in au, lower right plot) versus time (in yr) for $M_p = 1 M_N$, $r_p = 7$ au, $M_d = 10^{-2} M_\odot$, $R_i = 1$ au and $I_0 = 50^\circ$ (solid line) and 20° (dotted line). For these parameters, $I_c = 23^\circ$. When $I_0 = 20^\circ$, $e = 0$ throughout the evolution so the curve does not show on the plot. The Kozai effect provides a way of pumping up e and maintaining either e or I at large values, and therefore delays circularization and alignment with the disc of the orbit.

3.2.1 Influence of the planet's mass:

We now study the influence of the planet's mass on the evolution of the orbit. Figure 5 shows the time evolution of the inclination I , eccentricity e and semimajor axis a for the same parameters as in figure 4, i.e. $r_p = 7$ au, $M_d = 10^{-2} M_\odot$, $R_i = 1$ au, $I_0 = 50^\circ$ and three different values of M_p . As $I_c = 23^\circ$ for these parameters, we are in the regime where Kozai cycles are present. As shown by equation (15), the damping timescale τ_{damp} is proportional to $1/M_p$. The period P_{osc} of the Kozai cycle, on the other hand, does not depend on the planet's mass (see eq. [8] and [9]). We therefore expect friction to be very efficient for high mass planets for which the damping timescale τ_{damp} would be smaller than P_{osc} , and much

less efficient for low mass planets for which $\tau_{\text{damp}} \gg P_{\text{osc}}$. This is borne out by the results displayed in figure 5. Friction dominates the evolution for the planet with $M_p = 10 M_J$, for which τ_{damp} is smaller than P_{osc} . For a Jupiter mass planet, the two timescales are comparable and the orbit aligns after a few oscillations, i.e. after a few 10^5 years. For a Neptune mass planet, $\tau_{\text{damp}} \gg P_{\text{osc}}$ and I decreases very slowly. In that case, the orbit would stay misaligned over the disc lifetime.

As stated above, P_{osc} does not depend on the planet's mass. However, we see from figure 5 that the oscillations for $M_p = 1 M_J$ and $M_p = 1 M_N$ do not have the same period. This is because, as noted above, P_{osc} decreases as damping reduces the amplitude of the oscillations.

The fact that dynamical drag leads to faster alignment of the orbits for more massive planets was seen in the numerical simulations of Rein (2012) who considered planets on highly inclined orbits but without taking into account the gravitational interaction with the disc.

3.2.2 Influence of the disc's mass:

Figure 6 shows the time evolution of the inclination I and semimajor axis a for $M_p = 1 M_N$, $r_p = 7$ au, $R_i = 1$ au, $I_0 = 50^\circ$ (as in fig. 4) and three different values of M_d ranging from 10^{-2} to $0.1 M_\odot$. Terquem & Ajmia (2010) showed that I_c does not depend on M_d when the other parameters are kept fixed, so that we have $I_c = 23^\circ$ here. Since $I_0 = 50^\circ$, we are therefore in the regime of Kozai cycles. From equation (15), we see that $\tau_{\text{damp}} \propto M_d^{-1}$. On the other hand, we also have $P_{\text{osc}} \propto M_d^{-1}$, as expected from the classical Kozai effect and verified in the disc's case by Terquem & Ajmia (2010). It follows that alignment of the orbit with the disc, when it occurs, should happen after the same number of oscillations whatever the disc's mass. This is confirmed by the curves in figure 6 which are all a time-scaled version of each other, with the more massive disc showing the shortest evolution timescale. It is therefore easier to keep a planet on an inclined orbit in the presence of a less massive disc.

3.2.3 Influence of the planet's initial semimajor axis:

Finally, we study the effect of the initial semimajor axis on the orbital evolution. Figure 7 shows the time evolution of the inclination I for $M_p = 1 M_J$, $M_d = 10^{-2} M_\odot$, $R_i = 10$ au, $I_0 = 60^\circ$ and four different values of r_p ranging from 5 to 20 au. For these parameters, we

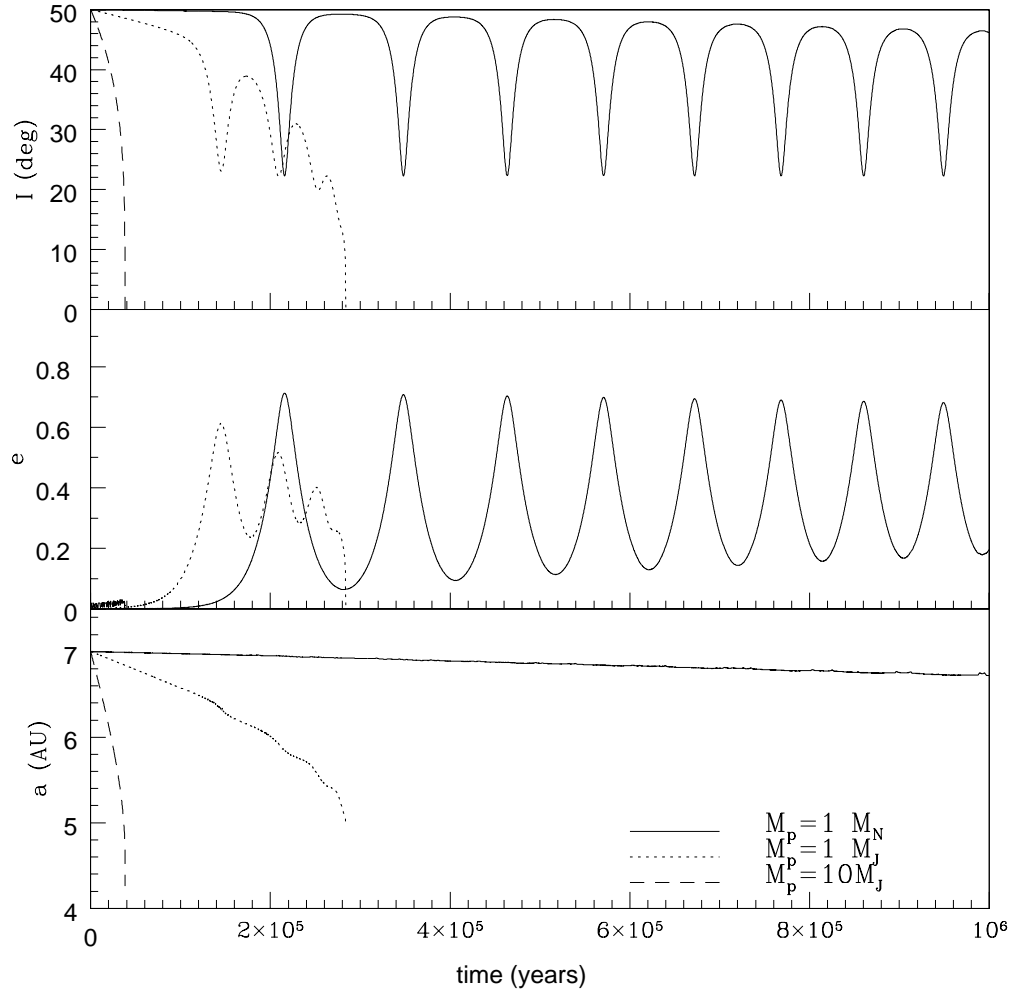


Figure 5. Inclination I (in degrees, upper plot), eccentricity (middle plot) and semimajor axis a (in au, lower plot) versus time (in yr) for $r_p = 7$ au, $M_d = 10^{-2} M_\odot$, $R_i = 1$ au, $I_0 = 50^\circ$ (same parameters as in fig. 4) and $M_p = 1 M_N$ (solid line), $1 M_J$ (dotted line) and $10 M_J$ (dashed line). For these parameters, $I_c = 23^\circ < I_0$ so that we are in the regime where Kozai cycles are present. Friction damps the oscillations more efficiently for larger mass planets. Alignment of the orbit with the disc may not happen over the disc lifetime for smaller mass planets.

are in the regime of Kozai cycles. For $r_p = 5$ au, the planet stays in the disc's inner cavity so that it never experiences frictional forces when it goes through the disc's plane. The orbital evolution is therefore that of a Kozai cycle with no friction and a minimum angle of 37° , consistent with the results of figure 3. For $r_p = 8$ au, although the distance to the star does get larger than R_i when $e > 0.25$, as it happens the planet is always in the disc's inner cavity when it crosses the disc's plane, so that here again friction does not play a role. Like in the previous case, the minimum angle for this cycle is consistent with the results of figure 3. As noted above, $P_{\text{osc}} \propto a^{-3/2}$ in the classical Kozai case. We verify here that P_{osc} does indeed decrease when a increases (in agreement with Terquem & Ajmia 2010). For $r_p = 12$ and

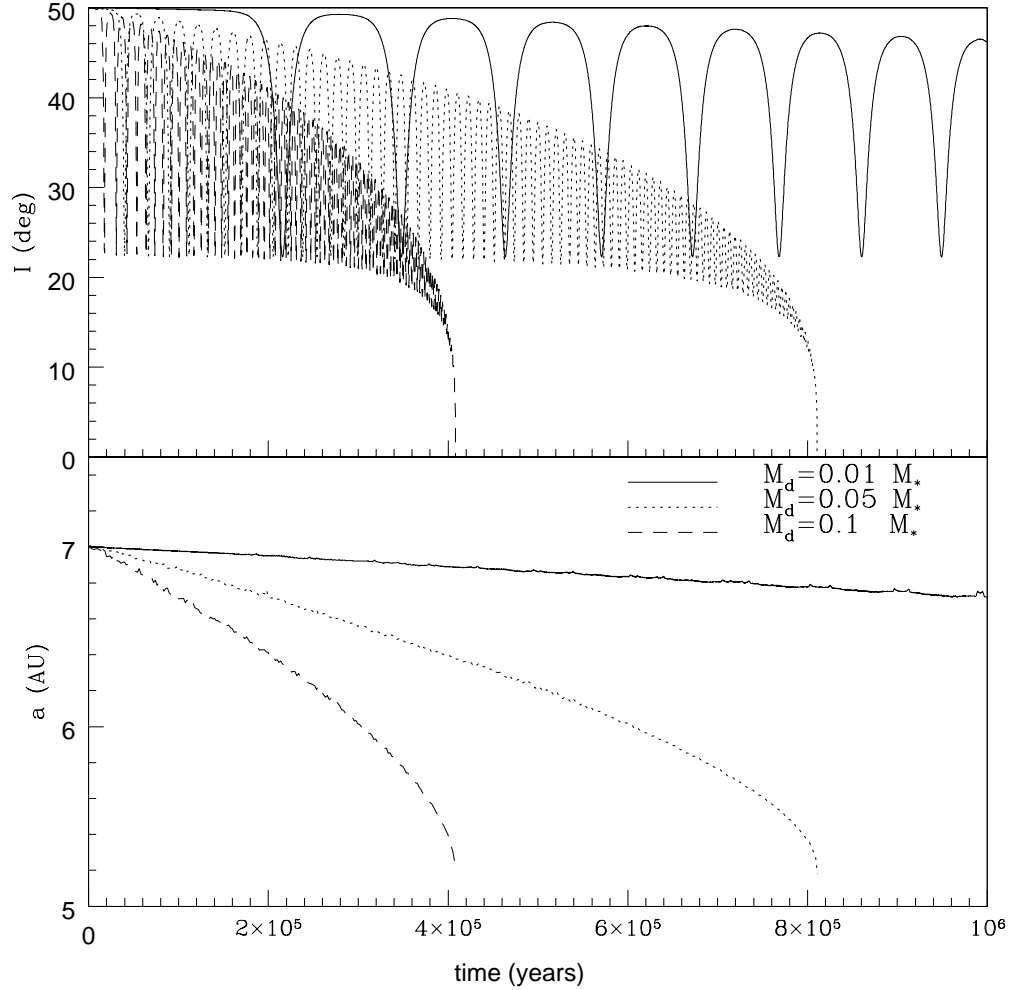


Figure 6. Inclination I (in degrees, upper plot) and semimajor axis a (in au, lower plot) versus time (in yr) for $M_p = 1 M_N$, $r_p = 7$ au, $R_i = 1$ au, $I_0 = 50^\circ$ (same parameters as in fig. 4) and $M_d = 0.1 M_\odot$ (dashed line), $5 \times 10^{-2} M_\odot$ (dotted line) and $10^{-2} M_\odot$ (solid line). For these parameters, $I_c = 23^\circ < I_0$ so that we are in the regime where Kozai cycles are present. It is easier to keep a planet on an inclined orbit in the presence of a less massive disc.

20 au, the planet crosses the disc so that the oscillations are damped by the frictional force. As shown by equation (15), the damping timescale τ_{damp} does not depend on a . This is consistent with the curves displayed in figure 7 at early times, before the eccentricity of the orbits grow, as they show that the damping timescale is indeed the same for $r_p = 12$ and 20 au. But as the inclination gets smaller for the larger value of r_p (I_{min} is smaller and the planet spends more time in the disc), τ_{damp} gets also shorter for this value of r_p . Alignment of the orbit with the disc is then faster at larger distances from the star.

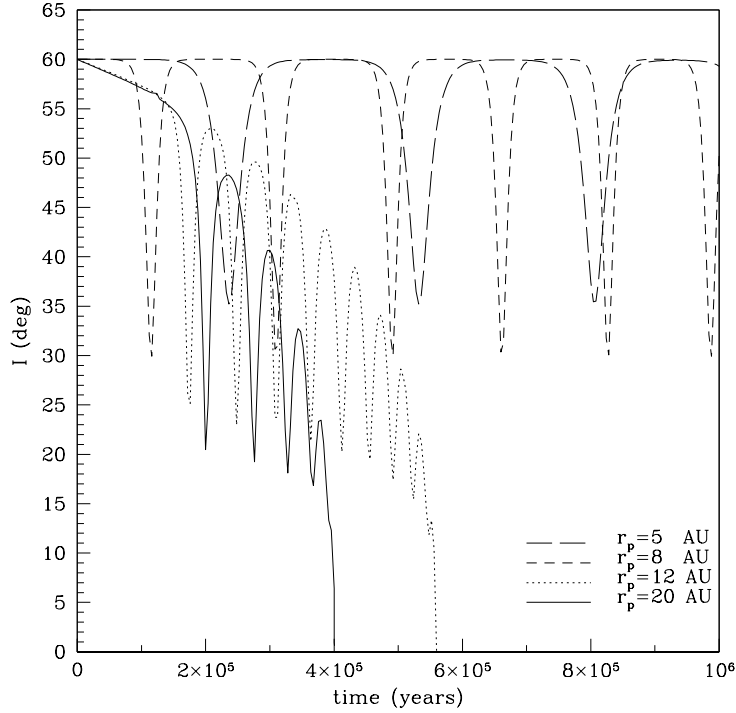


Figure 7. Inclination I (in degrees) versus time (in yr) for $M_p = 1 M_J$, $M_d = 10^{-2} M_\odot$, $R_i = 10$ au, $I_0 = 60^\circ$ and $r_p = 20$ au (solid line), 12 au (dotted line), 8 au (short dashed line) and 5 au (long dashed line). For these parameters, we are in the regime of Kozai cycles. Alignment of the orbit with the disc is faster at larger distances from the star.

4 DISCUSSION

We have investigated the dynamics of a planet on an orbit inclined with respect to a disc. If the initial inclination of the orbit is larger than some critical value, the gravitational force exerted by the disc on the planet leads to a Kozai cycle in which the eccentricity of the orbit is pumped up to large values and oscillates with time in antiphase with the inclination. On the other hand, when the planet goes through the disc, it suffers a frictional force that results in a loss of orbital energy. As a consequence, the inclination and the eccentricity of the orbit are damped and the semimajor axis decreases. The goal of this paper was to study on what timescale orbits inclined with respect to a disc would align with it.

The calculations presented in this paper show that, by pumping up the eccentricity of the planet's orbit and maintaining either I or e at large values, planets in orbits undergoing Kozai cycles maintain large velocities relative to the disc as they pass through it, so delaying alignment with the disc and circularization of the orbit.

For the parameters used in this paper, which are typical of protostellar discs, it was found that Neptune mass planets would remain on inclined orbits over the disc lifetime. Jupiter mass planets, however, tend to align faster, as the damping timescale is shorter for more

massive planets. Note however that we have not taken into account the fact that the disc dissipates progressively over time. As damping is less efficient in less massive discs, Jupiter mass planets could remain misaligned if the disc's mass were decreasing sufficiently fast. We have also found that alignment of the orbits was faster at larger distances from the star.

So far, the only planets that have been found on inclined orbits are rather massive (with a mass $\sim M_J$) and on short period orbits. This of course is a result of observational bias, as the inclination is measured so far only for transiting planets. As the results of this paper suggest, if these planets had been on inclined orbits when the disc was present, they probably would have aligned if they had crossed the disc. Therefore, either (i) the orbits became inclined after the disc had dissipated, (ii) the disc in which the planets formed was misaligned with the stellar equatorial plane, or (iii) the planets formed on inclined orbits with short enough periods that they crossed the disc's plane only in an inner cavity. Jupiter mass planets formed on inclined orbits at large distances from the star would be expected to have aligned with the disc unless the formation took place near the end of the life of the disc.

The planets in the Kepler sample seem to have both low inclinations (Fabrycky et al. 2012) and low eccentricities (Kane et al. 2012). Radial velocity surveys also show lower eccentricities for lower mass planets. According to the results of our paper, this strongly suggests that these planets, with masses mainly at most $\sim M_N$, have formed and stayed in the original disc. Had they been in a sufficiently inclined orbit at some point, this would have recurred over the disc lifetime, and the orbit would have had episodes of high eccentricity. Thus a population in both highly eccentric and inclined orbits would be expected. Measurement of inclination angles for longer period orbits will enable the evaluation of proposed aspects of planet formation scenarios.

Finally, we remark that in the present paper we have considered only one planet interacting with the disc. In a subsequent paper, we will investigate the dynamics of multiple systems.

REFERENCES

- Adams, F. C. and Laughlin, G., 2003, *Icarus*, 163, 290A
 Albrecht, S., Winn, J. N., Johnson, J. A., Howard, A. W., Marcy, G. W., Butler, R. P., Arriagada, P., Crane, J. D., Shectman, S. A., Thompson, I. B., Hirano, T., Bakos, G., Hartman, J. D., 2012, *astro-ph/1206.6105*
 Batalha, N. M. et al. 2012, *astro-ph/1202.5852*
 Bate M. R., Lodato G., Pringle J. E., 2010, *MNRAS*, 401, 1505

- Binney, J. and Tremaine, S., 1987 Galactic dynamics, Princeton University Press
- Borucki, W. J. et al. 2011, ApJ, 736, 19B
- Chatterjee S., Ford E. B., Matsumura S., Rasio F. A., 2008, ApJ, 686, 580
- Fabrycky D. C. et al. 2012, astro-ph/1202.6328
- Fabrycky D. C., Tremaine S., 2007, ApJ, 669, 1298
- Foucart F., Lai D., 2011, MNRAS, 412, 2799
- Innanen, K. A. and Zheng, J. Q. and Mikkola, S. and Valtonen, M. J., 1997 AJ, 113, 1915I
- Johns-Krull C. M., McCullough P. R., Burke C. J., Valenti J. A., Janes K. A., Heasley J. N., et al., 2008, ApJ, 677, 657
- Kane, S. R. and Ciardi, D. R. and Gelino, D. M. and von Braun, K., 2012, astro-ph/1203.1631
- Kozai Y., 1962, Astron. J., 67, 591
- Lai D., Foucart F., Lin D. N. C., 2011, MNRAS, 412, 2790
- Larwood J. D., Nelson R. P., Papaloizou J. C. B., Terquem C., 1996, MNRAS, 282, 597
- Lidov M. L., 1962, Planetary Space Science, 9, 719
- Naoz S., Farr W. M., Lithwick Y., Rasio F. A., Teyssandier J., 2011, Nature, 473, 187
- Nelson R. P., Papaloizou J. C. B., 1999, MNRAS, 309, 929
- Ostriker E. C., 1999, ApJ, 513, 252
- Papaloizou J. C. B., Terquem C., 1995, MNRAS, 274, 987
- Papaloizou J. C. B., Terquem C., 2001, MNRAS, 325, 221
- Press, W. H. and Teukolsky, S. A. and Vetterling, W. T. and Flannery, B. P., 1993, Numerical recipes in Fortran, Cambridge Univ. Press
- Rein H., 2012, MNRAS, 422, 3611
- Rephaeli, Y. and Salpeter, E. E., 1980, ApJ, 240, 20R
- Ruderman, M. A. and Spiegel, E. A., 1971, ApJ, 165, 1R
- Terquem C., Ajmia A., 2010, MNRAS, 404, 409
- Terquem C., Papaloizou J. C. B., 2002, MNRAS, 332, L39
- Thies I., Kroupa P., Goodwin S. P., Stamatellos D., Whitworth A. P., 2011, MNRAS, 417, 1817
- Watson C. A., Littlefair S. P., Diamond C., Collier Cameron A., Fitzsimmons A., Simpson E., Moulds V., Pollacco D. 2011, MNRAS, L413, 71
- Winn J. N., Holman M. J., Torres G., McCullough P., Johns-Krull C., et al., 2008, ApJ, 683, 1076
- Wu Y., Murray N. W., Ramsahai J. M., 2007, ApJ, 670, 820
- Wu Y., Lithwick Y., 2011, ApJ, 735, 109

APPENDIX A: RESPONSE OF THE DISC TO THE GRAVITATIONAL INTERACTION WITH THE PLANET

We here estimate the warping response of a disc of the type we consider to a planet in an inclined circular orbit. The disc is assumed to contain significantly more angular momentum than the planet and obey a barotropic equation of state. We show that provided the inverse of the orbital precession frequency is less than the local disc sound crossing time and the mass of the planet is less than the disc mass in its neighbourhood, the range of inclinations excited is expected to be small.

A1 Governing equations

The basic governing equations are the equations of continuity and motion for a barotropic gas in the form

$$\frac{\partial \rho}{\partial t} + \nabla \cdot \rho \mathbf{v} = 0, \quad (\text{A1})$$

$$\frac{\partial \mathbf{v}}{\partial t} + \mathbf{v} \cdot \nabla \mathbf{v} = -\frac{1}{\rho} \nabla P - \nabla \Phi - \nabla \Phi_*, \quad (\text{A2})$$

where $\Phi_* = -GM_*/|\mathbf{r}|$ is the gravitational potential due to the central star and

$$\Phi = -\frac{GM_p}{\sqrt{r^2 + R^2 - 2rR \cos(\phi - \phi_p) + (z - z_p)^2}} \quad (\text{A3})$$

is the potential due to the planet which is treated as a perturbation for which we calculate the linear response below (the indirect term does not contribute to the warping and so may be dropped). Here the cylindrical coordinates of the planet are (R, ϕ_p, z_p) .

We adopt a Fourier decomposition in azimuth and time of the form

$$\Phi = \sum_{m>0} \Phi_m \exp[i(m\phi + \omega_{p,m}t)] + cc, \quad (\text{A4})$$

where $+cc$ indicates the addition of the complex conjugate, m is the azimuthal mode number and $\omega_{p,m}$ is an associated frequency corresponding to a pattern speed $-\omega_{p,m}/m$. For global warps we are interested in $m = 1$ and pattern speeds that correspond to a slow precession of the planetary orbit. The precession period of the line of nodes, which for the purposes of this section is assumed to be given, is related and comparable to the period of Kozai oscillations when these occur. We adopt the time or orbit average of the coefficient Φ_1 which is appropriate for a discussion of the secular evolution of global warps. We perform a corresponding Fourier decomposition for the response perturbations to the disc which are taken to have a ϕ and t dependence through a multiplicative factor $\exp[i(m\phi + \omega_{p,m}t)]$. From now on this factor will be taken as read and we drop the subscript m on quantities as this is taken to be unity.

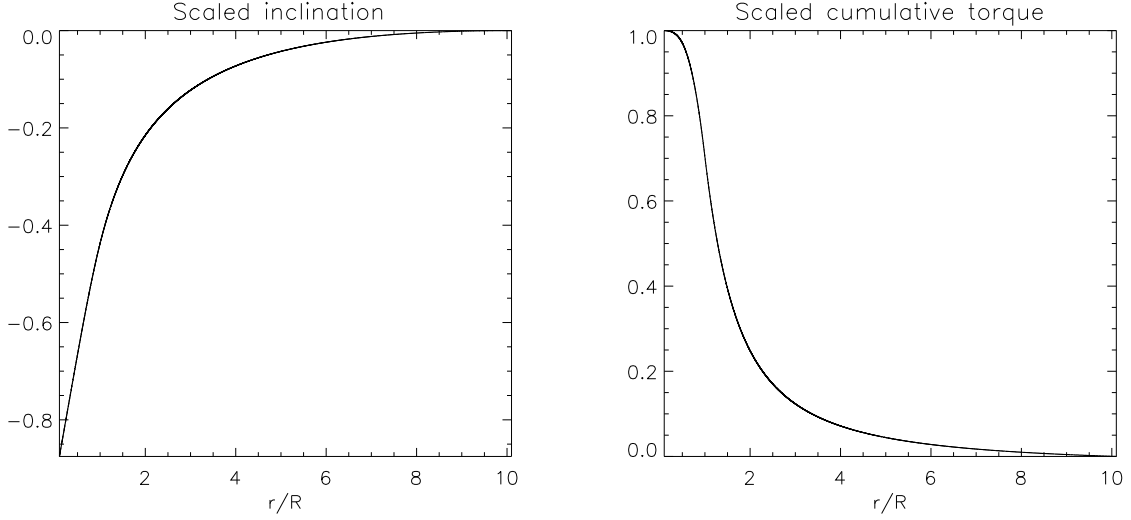


Figure A1. The left hand panel shows the inclination, normalized by the factor $10^3(M_p/M_*)(0.05R/H(R))^2\omega_p R^{3/2}/\sqrt{GM_*}$, as a function of r/R for the calculation described in the text. This was calculated under the condition that it tended to zero as $r \rightarrow \infty$. The right hand panel shows the function $T(r/R)/T(0)$ which represents the magnitude of the torque due to the planet acting on the disc in the radial interval (r, ∞) normalized by its value as $r \rightarrow 0$. For both panels the inclination of the circular planetary orbit of radius R to the plane of the disc was $\pi/4$.

A2 The disc inclination response

Denoting perturbations with a prime, linearization of the equations of motion (A2) for the response to the perturbing potential, Φ , gives

$$\begin{aligned} i(\omega_p + \Omega)v'_r - 2\Omega v'_\phi &= -\frac{\partial W}{\partial r} \\ i(\omega_p + \Omega)v'_\phi + \frac{\kappa^2}{2\Omega}v'_r &= -\frac{iW}{r} \\ i(\omega_p + \Omega)v'_z &= -\frac{\partial W}{\partial z} \end{aligned} \quad (\text{A5})$$

where $W = P'/\rho + \Phi$ and κ is the epicyclic frequency. Solving for the velocity perturbations, we obtain

$$\begin{aligned} v'_r &= -i \frac{(\omega_p + \Omega)\partial W/\partial r + 2\Omega W/r}{\kappa^2 - (\omega_p + \Omega)^2} \\ v'_\phi &= \frac{(\kappa^2/(2\Omega))\partial W/\partial r + (\omega_p + \Omega)W/r}{\kappa^2 - (\omega_p + \Omega)^2} \end{aligned} \quad (\text{A6})$$

As we are interested in a disc that is close to Keplerian rotation, with $\omega_p \ll \Omega$, and $\kappa \sim \Omega$, we neglect ω_p and set $\kappa = \Omega$ in the numerators above, and replace $\kappa^2 - (\omega_p + \Omega)^2$ by $2\Omega(\kappa - \omega_p - \Omega)$ in the denominators to obtain

$$\begin{aligned} v'_r &= -i \frac{\partial W/\partial r + 2W/r}{2(\kappa - \omega_p - \Omega)} \\ v'_\phi &= \frac{\partial W/\partial r + 2W/r}{4(\kappa - \omega_p - \Omega)} \end{aligned} \quad (\text{A7})$$

Following our previous work (eg Papaloizou & Terquem 1995, Larwood et al. 1996, Nelson & Papaloizou 1999) we seek a solution for which v'_z is independent of z to within a correction of order $(H/r)^2$. Then to within the same order of accuracy we may integrate the linearized z component of the equation of motion to give

$$W = -i(\omega_p + \Omega)zv'_z. \quad (\text{A8})$$

We now write down the linearized continuity equation in the form

$$\frac{i(\omega_p + \Omega)\rho(W - \Phi)}{c_s^2} = -\nabla \cdot (\rho \mathbf{v}'), \quad (\text{A9})$$

where we have used $P' = c_s^2 \rho'$, with $c_s^2 = dP/d\rho$. Multiplying (A9) by z and integrating over the vertical extent of the disc, we get

$$\int_{-\infty}^{\infty} \frac{i(\omega_p + \Omega)\Phi \rho z}{c_s^2} dz = \int_{-\infty}^{\infty} \frac{(\omega_p + \Omega)^2 v'_z \rho z^2}{c_s^2} dz - \int_{-\infty}^{\infty} v'_z \rho dz + \nabla_{\perp} \cdot \left(\int_{-\infty}^{\infty} z \mathbf{v}'_{\perp} \rho dz \right), \quad (\text{A10})$$

where the perpendicular velocity perturbation is $\mathbf{v}'_{\perp} = (v'_r, v'_{\phi}, 0)$. Making use of equations (A7), (A8) with ω_p neglected in the latter, and vertical hydrostatic equilibrium for the unperturbed state, we obtain

$$\frac{\partial}{\partial r} \left(\frac{\mu \Omega}{\omega_p + \Omega - \kappa} \frac{\partial g}{\partial r} \right) + \frac{4\omega_p \Sigma g}{\Omega} = \frac{2ir^2}{GM_*} \int_{-\infty}^{\infty} \rho \frac{\partial \Phi}{\partial z} dz \sim \frac{2ir^2 \Sigma}{GM_*} \left(\frac{\partial \Phi}{\partial z} \right)_{z=0}, \quad (\text{A11})$$

where

$$\mu = \int_{-\infty}^{\infty} \rho z^2 dz, \quad (\text{A12})$$

$g = r^2 \Omega v'_z / (r^3 \Omega^2) \equiv v'_z / (r \Omega)$ and terms of order ω_p^2 have been neglected. Note that consistently with the approximations used here, where possible, we have adopted Keplerian rotation and taken $r^3 \Omega^2 = GM_*$ to be a constant in this expression. Thus $2g$ becomes the local inclination of the disc (the factor of two arises from the form of the Fourier decomposition (A4)). We remark that (A11) may also be written as

$$\frac{\partial}{\partial r} \left(\frac{\mu \Omega}{\omega_p + \Omega - \kappa} \frac{\partial g}{\partial r} \right) + \frac{4\omega_p \Sigma g}{\Omega} = \frac{1}{\pi GM_*} \frac{dT}{dr}, \quad (\text{A13})$$

where, for orbits with line of nodes coinciding with the y axis as considered below, T is the torque due to the planet acting on the disc in the radial interval (r, ∞) in the x direction. Thus $T \rightarrow 0$ as $r \rightarrow \infty$.

A3 Solution for the disc inclination

We wish to solve (A13) for the inclination of the disc induced by a planet on an inclined orbit. As the unforced problem has solutions consisting of long wavelength bending waves

propagating with a speed that is a multiple of the sound speed (Nelson & Papaloizou 1999), a complete solution requires knowledge of the complete structure of the disc including boundary details which are beyond the scope of the modelling in this paper. To deal with this situation we assume the disc extends to large radii and has a much larger angular momentum content than the planet. We then look for a solution for which the inclination response is localized away from large radii having $g \rightarrow 0$, and $dg/dr \rightarrow 0$, for $r \rightarrow \infty$. These solutions are in fact regular as $r \rightarrow 0$ for the power law discs we adopt here. However, inner boundary effects could possibly cause the excitation of a freely propagating bending wave that should be added. But this should not affect an estimate of the scale of the warping. To simplify matters further, we shall take $\kappa = \Omega$ as expected for a constant aspect ratio disc, under the gravitational potential due to a central point mass, and assume that ω_p/Ω is much less than H/r . The latter assumption, which is expected to lead to mild warping (eg Larwood et al. 1996 and see below) enables us to neglect the term $\propto g$ in equation (A13) which can then be easily integrated to give

$$\frac{\mu\Omega}{\omega_p} \frac{\partial g}{\partial r} = \frac{1}{\pi GM_*} T, \quad (\text{A14})$$

and accordingly

$$g = -\omega_p \int_r^\infty \frac{T}{\pi\mu\Omega GM_*} dr. \quad (\text{A15})$$

We make a rough estimate of g as determined by (A15) by setting $\mu = \Sigma H^2$ and $T \sim \pi G M_p \Sigma r \sim M_p r^2 \omega_p \Omega$, where r is evaluated at a location where the planet intersects the disc. Then we estimate

$$g \sim \frac{\omega_p M_p r^2}{\Omega M_* H^2} \sim \left(\frac{\omega_p^2 r^2}{\Omega^2 H^2} \right) \left(\frac{M_p \Omega}{M_* \omega_p} \right). \quad (\text{A16})$$

This implies that the inclination range is in general small. The first factor in brackets measures the square of the product of the precession frequency and local sound crossing time which is expected to be less than unity and so lead to only small warping (see Papaloizou & Terquem 1995, Larwood et al. 1996, Nelson & Papaloizou 1999). The second factor in brackets is expected to be the ratio of the planet mass to the characteristic disc mass contained within a length scale comparable to that of the orbit, which is expected to be less than of order unity particularly for low mass planets.

We have evaluated the solution given by (A15) for a planet in a circular orbit of radius R , inclined at 45 degrees to the plane of the disc and with line of nodes coinciding with the y axis. We took $\Sigma \propto r^{-1/2}$ as in the main text and as the solution scales with the inverse

square of the disc aspect ratio, H/r , that is left as a parameter. The left hand panel of Fig. A1 shows the inclination in units of $10^3(M_p/M_*)(0.05R/H(R))^2\omega_p R^{3/2}/\sqrt{GM_*}$, as a function of r/R . The maximum value of this is of order unity indicating that, even for a Jovian mass planet in a disc with aspect ratio 0.05, the characteristic value of the inclination range is of order $\omega_p R^{3/2}/\sqrt{GM_*}$ which is expected to be of the order of the ratio of the mass of the disc to that of the central star and thus a small quantity. The right hand panel of Fig. A1 shows the cumulative torque $T(r/R)/T(0)$ measured in the sense of increasing inwards. This indicates that the torque falls off rapidly at large radii.

APPENDIX B: EXPRESSION OF THE GRAVITATIONAL FORCE DUE TO THE DISC IN TERMS OF ELLIPTIC INTEGRALS

Here we develop expressions for the gravitational force per unit mass exerted by a disc on a planet that may be passing through it in terms of elliptic integrals. The resulting expressions require the evaluation of two dimensional integrals with integrands that at worst contain a logarithmic singularity which is readily manageable numerically.

The gravitational potential exerted by the disk at the location (r, z) of the planet is given by equation (1) as

$$\Phi(r, z_p) = -G \int_{R_i}^{R_o} \int_{-H}^H \int_0^{2\pi} \frac{\rho(r', z') r' dr' dz' d\phi'}{\sqrt{r^2 + r'^2 - 2rr' \cos \phi' + (z - z')^2}}, \quad (\text{B1})$$

As the disc is axisymmetric, the gravitational force per unit mass exerted by the disc on the planet has only a radial and a vertical components, given by $-\partial\Phi/\partial r$ and $-\partial\Phi/\partial z$, respectively. To calculate these, we first note that Φ is solution of Poisson's equation, which is given by

$$\frac{\partial^2 \Phi}{\partial r^2} + \frac{1}{r} \frac{\partial \Phi}{\partial r} + \frac{\partial^2 \Phi}{\partial z^2} - \frac{m^2 \Phi}{r^2} = 4\pi G \rho(r, z), \quad (\text{B2})$$

with $m = 0$. In the general nonaxisymmetric case, when the φ dependence of ρ is through a factor $\exp(i\varphi)$, the azimuthal number m is nonzero and we have $\partial^2 \Phi / \partial \varphi^2 = -m^2 \Phi$. We now differentiate equation (B2), with $m = 0$, with respect to r to obtain to

$$\frac{\partial^2}{\partial r^2} \left(\frac{\partial \Phi}{\partial r} \right) + \frac{1}{r} \frac{\partial}{\partial r} \left(\frac{\partial \Phi}{\partial r} \right) - \frac{1}{r^2} \frac{\partial \Phi}{\partial r} + \frac{\partial^2}{\partial z^2} \left(\frac{\partial \Phi}{\partial r} \right) = 4\pi G \frac{\partial \rho}{\partial r}. \quad (\text{B3})$$

This shows that $\partial\Phi/\partial r$ satisfies Poisson's equation with $m = 1$ and $\partial\rho/\partial r$ as source term. The solution can be written as

$$\frac{\partial \Phi}{\partial r} = -G \int_{R_i}^{R_o} \int_{-H}^H \int_0^{2\pi} \frac{\frac{\partial \rho}{\partial r}(r', z') r' dr' \cos \phi' dz' d\phi'}{\sqrt{r^2 + r'^2 - 2rr' \cos \phi' + (z - z')^2}} + B_i + B_o. \quad (\text{B4})$$

Here the domain of integration is the interior of the domain containing the mass distribution and B_i and B_o are boundary terms that have to be taken into account when the disc's mass density is given by equation (2), as in that case $\partial \rho / \partial r$ is infinite at the radial boundaries of the disc. When the disc's mass density is made continuous by multiplication by the factor f defined in equation (3), these boundary terms are not included.

Expression (B4) can be recast in the form:

$$\frac{\partial \Phi}{\partial r} = -G \int_{R_i}^{R_o} \int_{-H}^H \frac{\partial \rho}{\partial r}(r', z') H_r(r, r', z - z') r' dr' dz' + B_i + B_o, \quad (\text{B5})$$

with

$$H_r(r, r', z - z') = \int_0^{2\pi} \frac{\cos \phi' d\phi'}{\sqrt{r^2 + r'^2 - 2rr' \cos \phi' + (z - z')^2}}. \quad (\text{B6})$$

We define $a^2 = r^2 + r'^2 + (z - z')^2$, $b^2 = 2rr'$ and $u = 2b^2/(a^2 + b^2)$. It is then straightforward to show that:

$$H_r(r, r', z - z') = \frac{4\sqrt{a^2 + b^2}}{b^2} \left[\frac{a^2}{a^2 + b^2} K(u) - E(u) \right], \quad (\text{B7})$$

where K and E are the elliptic integrals of the first and second kind, defined as:

$$K(m) = \int_0^{\pi/2} \frac{d\theta}{\sqrt{1 - m \sin^2 \theta}}, \quad (\text{B8})$$

$$E(m) = \int_0^{\pi/2} \sqrt{1 - m \sin^2 \theta} d\theta, \quad (\text{B9})$$

with $m < 1$.

We calculate the boundary terms B_i and B_o by assuming that ρ is continuous and supposing that ρ increases from 0 to $\rho(R_i, z)$ over a distance $\Delta r \rightarrow 0$ at the inner edge, and decreases from $\rho(R_o, z)$ to 0 over the same distance at the outer edge, i.e.:

$$B_i = -G \int_{R_i - \Delta r}^{R_i} \int_{-H}^H \frac{\partial \rho}{\partial r}(r', z') H_r(r, r', z - z') r' dr' dz', \quad (\text{B10})$$

$$= -G \int_{-H(R_i)}^{H(R_i)} \rho(R_i, z') R_i H_r(r, R_i, z - z') dz'. \quad (\text{B11})$$

Similarly:

$$B_o = -G \int_{R_o}^{R_o+\Delta r} \int_{-H}^H \frac{\partial \rho}{\partial r}(r', z') H_r(r, r', z - z') r' dr' dz', \quad (\text{B12})$$

$$= +G \int_{-H(R_o)}^{H(R_o)} \rho(R_o, z') R_o H_r(r, R_o, z - z') dz'. \quad (\text{B13})$$

We calculate $\partial\Phi/\partial z$ in a similar way by differentiating Poisson's equation (B2), with $m = 0$, with respect to z , which leads to:

$$\frac{\partial^2}{\partial r^2} \left(\frac{\partial\Phi}{\partial z} \right) + \frac{1}{r} \frac{\partial}{\partial r} \left(\frac{\partial\Phi}{\partial z} \right) + \frac{\partial^2}{\partial z^2} \left(\frac{\partial\Phi}{\partial z} \right) = 4\pi G \frac{\partial \rho}{\partial z}. \quad (\text{B14})$$

This shows that $\partial\Phi/\partial z$ satisfies Poisson's equation with $m = 0$ and $\partial\rho/\partial z$ as source term.

The solution can be written as

$$\frac{\partial\Phi}{\partial z} = -G \int_{R_i}^{R_o} \int_{-H}^H \int_0^{2\pi} \frac{\frac{\partial \rho}{\partial z}(r', z') r' dr' d\phi' dz'}{\sqrt{r^2 + r'^2 - 2rr' \cos \phi' + (z - z')^2}}. \quad (\text{B15})$$

This expression can be recast in the form

$$\frac{\partial\Phi}{\partial z} = -G \int_{R_i}^{R_o} \int_{-H}^H \frac{\partial \rho}{\partial z}(r', z') H_z(r, r', z - z') r' dr' dz', \quad (\text{B16})$$

with:

$$H_z(r, r', z - z') = \int_0^{2\pi} \frac{d\phi'}{\sqrt{r^2 + r'^2 - 2rr' \cos \phi' + (z - z')^2}}, \quad (\text{B17})$$

or, in term of the elliptic function K :

$$H_z(r, r', z - z') = \frac{4}{\sqrt{a^2 + b^2}} K(u). \quad (\text{B18})$$